Article

Ab Initio Study of the Mechanism for Photoinduced Yl-Oxygen Exchange in Uranyl(VI) in Acidic Aqueous Solution

Florent Re#al, Vale#rie Vallet, Ulf Wahlgren, and Ingmar Grenthe

J. Am. Chem. Soc., **2008**, 130 (35), 11742-11751 • DOI: 10.1021/ja8026407 • Publication Date (Web): 08 August 2008

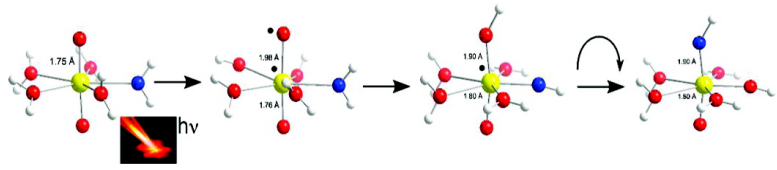

More About This Article

Additional resources and features associated with this article are available within the HTML version:

- Supporting Information
- Links to the 1 articles that cite this article, as of the time of this article download
- Access to high resolution figures
- Links to articles and content related to this article
- Copyright permission to reproduce figures and/or text from this article

View the Full Text HTML

J|A|C|S
ARTICLES

Published on Web 08/08/2008

Ab Initio Study of the Mechanism for Photoinduced Yl-Oxygen Exchange in Uranyl(VI) in Acidic Aqueous Solution

Florent Réal,[†,‡] Valérie Vallet,[*,‡] Ulf Wahlgren,[†,§] and Ingmar Grenthe[||]

Department of Physics, Stockholm University, AlbaNova University Centre, 106 91 Stockholm, Sweden, Université des Sciences et Technologies de Lille 1, Laboratoire PhLAM, CNRS UMR 8523, CERLA, CNRS FR 2416, Bât P5, 59655 Villeneuve d'Ascq Cedex, France, NORDITA, AlbaNova University Centre, 106 91 Stockholm, Sweden, and KTH Royal Institute of Technology, Inorganic Chemistry, SE-100 44 Stockholm, Sweden

Received April 10, 2008; E-mail: valerie.vallet@univ-lille1.fr

Abstract: The mechanism for the photochemically induced isotope-exchange reaction $U^{17/18}O_2^{2+}(aq) + H_2{}^{16}O \rightleftarrows U^{16}O_2^{2+}(aq) + H_2{}^{17/18}O$ has been studied using quantum-chemical methods. There is a dense manifold of states between 22 000 and 54 000 cm^{-1} that results from excitations from the σ_u and π_u bonding orbitals in the $^1\Sigma_g^+$ ground state to the nonbonding f_δ and f_ϕ orbitals localized on uranium. On the basis of investigations of the reaction profile in the $^1\Sigma_g^+$ ground state and the excited states $^3\Delta_g$ (the lowest triplet state) and $^3\Gamma_g$ (one of the several higher triplet states), the latter two of which have the electron configurations $\sigma_u f_\delta$ and $\pi_u f_\phi$, respectively, we suggest that the isotope exchange takes place in one of the higher triplet states, of which the $^3\Gamma_g$ state was used as a representative. The geometries of the luminescent $^3\Delta_g$ state, the lowest in the $\sigma_u f_{\delta,\phi}$ manifold (the "σ" states), and the $^1\Sigma_g^+$ ground state are very similar, except that the bond distances are slightly longer in the former. This is presumably a result of transfer of a bonding electron to a nonbonding f orbital, which makes the excited state in some respects similar to uranyl(V). As is the case for all of the states of the $\pi_u f_{\delta,\phi}$ manifold (the "π" states), the geometry of the $^3\Gamma_g$ state is very different from that of the $^3\Delta_g$ "σ" state and has nonequivalent $U-O_{yl}$ distances of 1.982 and 1.763 Å; in the $^3\Gamma_g$ state, the yl-exchange takes place by transfer of a proton or hydrogen from water to the more distant yl-oxygen. The activation barriers for proton/hydrogen transfer in the ground state and the $^3\Delta_g$ and $^3\Gamma_g$ states are 186, 219, and 84 kJ/mol, respectively. The relaxation energy for the $^3\Gamma_g$ state in the solvent after photoexcitation is −86 kJ/mol, indicating that the energy barrier can be overcome; the "π" states are therefore the most probable route for proton/hydrogen transfer. They can be populated after UV irradiation but are too high in energy (∼36000−40000 cm^{-1}) to be reached by a single-photon absorption at 436 nm (22 900 cm^{-1}), where experimental data have demonstrated that exchange can take place. Okuyama et al. [*Bull. Res. Lab. Nucl. React. (Tokyo Inst. Technol.)* **1978**, *3*, 39–50] have demonstrated that an intermediate is formed when an acidic solution of $UO_2^{2+}(aq)$ is flash-photolyzed in the UV range. The absorption spectrum of this short-lived intermediate (which has a maximum at 560 nm) indicates that this species arises from 436 nm excitation of the luminescent $^3\Delta_g$ state (which has a lifetime of $\sim 2 \times 10^{-6}$ s); this is sufficient to reach the reactive "π" states. It has been speculated that the primary reaction in acidic solutions of $UO_2^{2+}(aq)$ is the formation of a uranyl(V) species; our results indicate that the structure in the luminescent state has some similarity to that of UO_2^+ but that the reactive species in the "π" states is a cation radical with a distinctly different structure.

Introduction

Photoexcitation in the UV range is used as a method to prepare $^{17/18}O_{yl}$-enriched $UO_2^{2+}(aq)$ from isotope-enriched water,[1] and in this article we will discuss the mechanism of this reaction. We have studied the corresponding thermal (or "dark") reaction in a previous investigation[2] using $^{17/18}O$ exchange between uranyl(VI) and water and suggested that the reaction involves proton/hydrogen transfer from coordinated water to the yl-oxygen, resulting in a $UO_{yl}(^{17/18}OH)_{yl}(OH)_{eq}$ unit in the binuclear hydroxide complex $(UO_2)_2(OH)_2^{2+}$ in which the equatorial (eq) and axial (yl) OH groups could change places. The equatorial OH group is labile, resulting in oxygen-isotope exchange with the water solvent. In the present theoretical study, we have explored whether a similar mechanism might also explain the photo-assisted exchange in strongly acidic solutions, where $UO_2^{2+}(aq)$ is the totally dominant species. Our first problem was to decide if the photoassisted exchange takes place in the luminescent triplet state or a higher excited state.

Much of the photochemistry of the uranyl ion has been focused on its electron configuration and the properties of its luminescent state; these studies date back to the days of the

[†] Stockholm University.
[‡] Université des Sciences et Technologies de Lille 1.
[§] NORDITA.
[||] KTH Royal Institute of Technology.

(1) Jung, W.-S.; Ikeda, Y.; Tomiyasu, H.; Fukutomi, H. *Bull. Chem. Soc. Jpn.* **1984**, *57*, 2317–2318.
(2) Szabó, Z.; Grenthe, I. *Inorg. Chem.* **2007**, *46*, 9372–9378.

 10.1021/ja8026407 CCC: $40.75

Becquerels,[3] and the progress has been described in monographs[4] and reviews.[5] These studies cover broad fields that include mechanisms of luminescence quenching and photoinduced redox reactions, but these will not be discussed in this article. Yusov and Shilov have provided an exhaustive discussion of the reactions of the photoexcited uranyl(VI) ion with water (see pp 1929−1932 of ref 5d), the main conclusion of which is that "no chemical changes are usually observed upon photo-irradiation of aqueous solutions of uranyl salts containing no reducing agents."

There are two main proposals about the primary photochemical processes (stars denote photoexcited or radical states):

- formation of uranyl(V) and a hydroxide radical[6] from the photoexcited state according to the reaction

$$[UO_2^{2+}]^* + H_2O \rightleftarrows UO_2^{+} + OH^{\bullet} + H^{+} \quad (1)$$

- hydrogen abstraction and simultaneous formation of a $OH^{\bullet}$ radical[5d,7] according to the reaction

$$[UO_2^{2+}]^* + H_2O \rightleftarrows [UO_2H^{2+}]^* + OH^{\bullet} \quad (2)$$

Most experimental investigations have used excitation at 300−450 nm (22000−33000 cm^{-1}), and it is commonly assumed that the photochemical reactions take place in the luminescent state (see p 1926 of ref 5d).

The nature of the $U-O_{yl}$ bonding is important for the discussion of the photochemical reactions: in the ground state, the bonds are strong and usually chemical inert, except in $(UO_2)_2(OH)_2^{2+}$ and other polynuclear hydroxide complexes;[2] on photoexcitation, the bonding is weaker, and accordingly, the UO_2 group is chemically more reactive.

For the following discussion, it is necessary to begin with a short summary of the electronic structures of the ground and excited electronic states of the uranyl(VI) ion as deduced from previous spectroscopic and quantum-chemical studies.[8–12] In one of these studies,[12] we calculated the energy levels of UO_2^{2+} and its structure and electron distribution in both ground and excited states using quantum-chemical methods; we used the common spectroscopic notation for the various levels, even though there is extensive spin−orbit coupling in these systems. An important observation in our previous study was that the distances between uranium and the yl-oxygens were not equivalent in the $^3\Pi_g$ and $^3\Gamma_g$ excited states, in contrast to the equal bond distances in the $^1\Sigma_g^+$ ground state and the $^3\Delta_g$, $^1\Delta_g$, $^3\Phi_g$ and $^1\Phi_g$ excited states. The different geometries in various excited states might influence proton/hydrogen transfer from water to uranyl oxygen and the subsequent isotope exchange with water.

There is a dense manifold of states between 22 000 and 54 000 cm^{-1} that results from excitations from the uranyl σ_u, σ_g, π_g, and π_u bonding orbitals to the nonbonding f_δ and f_ϕ orbitals localized on the uranium atom; the order of the different energy levels is given in Tables I and II of ref 12. The first excited state of uranyl(VI), $^3\Delta_g(\sigma_u f_\delta)$, which is produced by excitation from a bonding σ_u orbital into an f_δ orbital, has a symmetric equilibrium geometry with a $U-O_{yl}$ distance 0.06 Å longer than that in the electronic ground state. The dipole transition to this electronic state is forbidden both by parity and spin. As discussed in Chemical Models and Computational Methods, the gerade/ungerade symmetries may disappear in the solution phase, allowing the dipole transition to become weakly allowed by both symmetry-breaking and spin−orbit effects. This accounts for the luminescent character of this state and for the long lifetime of several microseconds. Higher (vertical) gerade electronic states arising from excitations out of the π_u orbitals have asymmetric relaxed structures as a result of charge separation of the two unpaired electrons. The more distant oxygen atom acquires a radical character and most likely becomes a strong proton/hydrogen acceptor. In the near-UV range, the molar absorptivity is significantly larger than at longer wavelengths, and the vertical transition from the ground state presumably goes to one of the higher excited singlet states (see Table I of ref 12).

Previous experimental studies[5,13] have suggested that hydrogen abstraction can explain both fluorescence quenching and photochemical oxidation of different substrates. Mechanisms involving proton abstraction have not been discussed in detail, even though less energy is required to remove a proton than a hydrogen radical from water because the radical form is energetically less favored than the ionic form by ∼2 eV (193 kJ/mol).[14] Proton transfer has been suggested in mechanistic discussions by Okuyama et al.[15] and Gaziev et al.;[6b] we have studied this proposal both in the ground and excited states of the uranyl(VI) aqua ion using quantum-chemical methods. Because of complications that arise in geometry optimizations of excited states, we used simplified chemical and quantum-chemical models.

Chemical Models and Computational Methods

On the basis of differences in the $U-O_{yl}$ distances in the $^1\Sigma_g^+$, $^3\Delta_g(\sigma_u f_\delta)$, and $^3\Gamma_g(\pi_u f_\phi)$ states, we have explored the following:

- Two chemical models, the first with one coordinated water ligand in the coordination sphere and the second with five coordinated water ligands in the first and one in the second coordination sphere, schematically described by eqs 3 and 4, respectively, in which the star denotes the photoexcited state and the superscript "17/18" indicates isotope-enriched oxygen:

(3) Becquerel, E. *Ann. Chim. Phys.* **1859**, *57*, 102.
(4) (a) Rabinovich, E.; Belford, R. *Spectroscopy and Photochemistry of Uranyl Compounds*; Macmillan: New York, 1964. (b) *Gmelin Handbook of Inorganic Chemistry, Suppl. Ser. Uranium*; Springer Verlag: Berlin, 1983; Vol. A6, p 80.
(5) (a) Burrows, H. D.; Kemp, T. J. *Chem. Soc. Rev.* **1974**, *3*, 139–165. (b) Baird, C. P.; Kemp, T. J. *Prog. React. Kinet.* **1997**, *22*, 87–139. (c) Fazekas, Z.; Tomiyasu, H.; Park, Y.-Y.; Yamamura, T.; Harada, M. *ACH−Models Chem.* **1998**, *135*, 783. (d) Yusov, A. B.; Shilov, V. P. *Russ. Chem. Bull., Int. Ed.* **2000**, *49*, 1925–1953. (e) Denning, R. G.; Green, J. C.; Hutchings, T. E.; Dallera, C.; Giarda, K.; Brookes, N. B.; Braichovic, L. *J. Chem. Phys.* **2002**, *117*, 8008–8020.
(6) (a) Moriyasu, M.; Yokoyama, Y.; Ikeda, S. *J. Inorg. Nucl. Chem.* **1977**, *39*, 2211–2214. (b) Gaziev, S. A.; Gorshkov, N. G.; Mashirov, L. G.; Suglobov, D. N. *Inorg. Chim. Acta* **1987**, *139*, 345–351. (c) Formosinho, S. J.; Burrows, H. D.; da Graça Miguel, M.; Azenha, M. E. D. G.; Saraiva, I. M.; Ribeiro, A. C. D. N.; Khudyakov, I. V.; Gasanov, R. G.; Bolte, M.; Sarakha, M. *Photochem. Photobiol. Sci.* **2003**, *2*, 569–575.
(7) Burrows, H. D.; Formosinho, S. J. *J. Chem. Soc., Faraday Trans. 2* **1977**, *73*, 201–208.
(8) Denning, R. G. *J. Phys. Chem. A* **2007**, *111*, 4125–4143.
(9) Zhang, Z.; Pitzer, R. M. *J. Phys. Chem. A* **1999**, *103*, 6880–6886.
(10) Pierloot, K.; van Besien, E. *J. Chem. Phys.* **2005**, *123*, 204309.
(11) Pierloot, K.; van Besien, E.; van Lenthe, E.; Baerends, E. J. *J. Chem. Phys.* **2007**, *126*, 194311.
(12) Réal, F.; Vallet, V.; Marian, C. M.; Wahlgren, U. *J. Chem. Phys.* **2007**, *127*, 214302.
(13) Bouby, M.; Billard, I.; Bonnenfant, A.; Klein, G. *Chem. Phys.* **1999**, *240*, 353–370.
(14) Sobolewski, A. L.; Domcke, W. *J. Chem. Phys.* **2005**, *122*, 184320.
(15) Okuyama, K.; Ishikawa, Y.; Kato, Y.; Fukutomi, H. *Bull. Res. Lab. Nucl. React. (Tokyo Inst. Technol.)* **1978**, *3*, 39–50.

$$[U^{17/18}O_2(OH_2)^{2+}]^* + H_2O \rightleftarrows [UO_2(OH_2)^{2+}]^* + H_2{}^{17/18}O \quad (3)$$

$$[U^{17/18}O_2(OH_2)_5{}^{2+}]^* + H_2O \rightleftarrows [UO_2(OH_2)_5{}^{2+}]^* + H_2{}^{17/18}O \quad (4)$$

- Proton/hydrogen transfer to the yl-oxygen by calculation of the electronic energies of the different electron configurations as a function of the $O_{yl}-H$ distance, thereby identifying the transition state, the activation energy, and the energy of the "$UO_{yl}(OH)_{yl}$" intermediate.
- A mechanism leading to exchange between the yl- and water oxygens in eq 3 of the first model, which consists of the following steps:

$$[U^{17/18}O_2(OH_2)^{2+}]^* \rightleftarrows [UO_{yl}(^{17/18}OH)_{yl}(OH)_{eq}{}^{2+}]^* \quad (5)$$

$$[UO_{yl}(^{17/18}OH)_{yl}(OH)_{eq}{}^{2+}]^* \rightleftarrows [UO_{yl}(OH)_{yl}(^{17/18}OH)_{eq}{}^{2+}]^* \quad (6)$$

$$[UO_{yl}(OH)_{yl}(^{17/18}OH)_{eq}{}^{2+}]^* \rightleftarrows [UO_2(^{17/18}OH_2)^{2+}]^* \quad (7)$$

In contrast to the case in eq 1, the first step of the mechanism (eq 5) involves proton/hydrogen transfer from the coordinated water to one of the yl-oxygens. The second step (eq 6) involves the exchange of the axial and equatorial OH^- groups, which is followed by a proton/hydrogen transfer to the equatorial hydroxide group (eq 7). This step is followed by rapid exchange between water in the first hydration and the water solvent.[16] The corresponding mechanistic model for eq 4 involving the uranyl pentaaqua ion with water in the second coordination sphere is as follows:

$$[U^{17/18}O_2(OH_2)_5{}^{2+}]^*, (H_2O) \rightleftarrows [UO_{yl}(^{17/18}OH)_{yl}(OH)_{eq}(OH_2)_4{}^{2+}]^*, (H_2O) \quad (8)$$

$$[UO_{yl}(^{17/18}OH)_{yl}(OH)_{eq}(OH_2)_4{}^{2+}]^*, (H_2O) \rightleftarrows [UO_{yl}(OH)_{yl}(^{17/18}OH)_{eq}(OH_2)_4{}^{2+}]^*, (H_2O) \quad (9)$$

$$[UO_{yl}(OH)_{yl}(^{17/18}OH)_{eq}(OH_2)_4{}^{2+}]^*, (H_2O) \rightleftarrows [UO_2(^{17/18}OH_2)(OH_2)_4{}^{2+}]^*, (H_2O) \quad (10)$$

The water in the second coordination sphere acts as a "proton/hydrogen shuttle" (see Figure 5b and Figure S2b in the Supporting Information) for fast proton/hydrogen transfer reactions involving the solvent.

Choice of Computational Methods. Even with the simplified model, wave-function-based correlated methods, such as multireference configuration interaction (MRCI), and complete active space second-order perturbation theory (CASPT2) become complicated and time-consuming, in particular for higher excited states; we therefore resorted to the computationally less-demanding density functional theory (DFT) and time-dependent density functional theory (TD-DFT) methods. Five recent studies[10–12,17,18] have discussed the accuracy of these methods for geometries and excitation energies for the bare and coordinated uranyl ions. In general, CASPT2 gives excitation energies lower than those from the wave-function-based methods but still significantly higher than those from TD-DFT, particularly for the higher states (as shown in ref 12, a very large active space is necessary for accurate results in this region). The TD-DFT transition energies for the bare uranyl ion using the common B3LYP functional deviate by up to 12 000 cm^{-1} (144 kJ/mol) from the values obtained with accurate wave-function-based methods such as linear response coupled-cluster single and doubles (LR-CCSD) or size-extensive corrected multireference configuration interaction methods (MR-AQCC or MR-CI).[12] However, with respect to geometries, DFT and TD-DFT yield reasonably accurate bond distances and relaxation energies for all of the excited states, within 0.08 Å and 10 kJ/mol, respectively, of reference LR-CCSD values. We will base the following discussion on energetics obtained using the DFT/B3LYP and TD-DFT/B3LYP methods. For computational reasons, it was not realistic to use wave-function-based methods, and although the errors inherent in the DFT-based methods are significant, we expect some cancelation of errors in the calculation of reaction and transition-state energies. It should be emphasized that the differences in activation energies between the different states of interest are large (more than 180 kJ/mol) and that we thus are confident that the chemical conclusions are qualitatively correct.

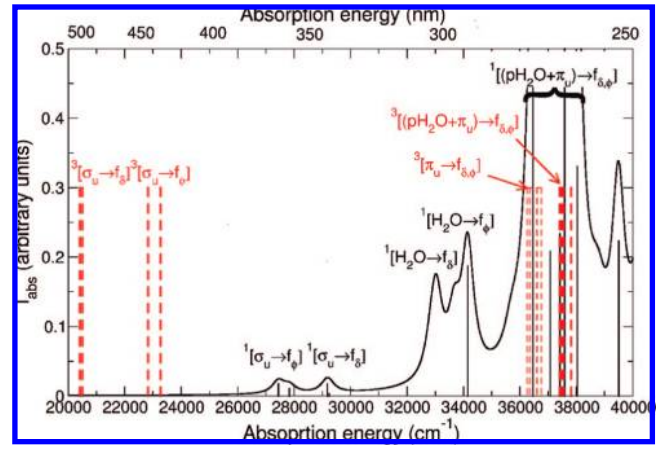

Figure 1. Absorption spectrum of the uranyl pentaaqua ion computed with TD-DFT/B3LYP without spin−orbit coupling. The theoretical stick spectrum of the singlet states (black lines) is convoluted with a Lorentzian function with a half-width at half-maximum of 500 cm^{-1}. The red sticks refer to the position of the triplet states. The intensities are scaled to set the maxima of the stick and convoluted spectra to 0.5 and 1.0, respectively. The computed transition energies and oscillator strengths are reported in Table S1 in the Supporting Information.

Excited States of the Uranyl(VI) Pentaaqua Ion. We computed the vertical absorption spectrum of the uranyl pentaaqua ion, $UO_2(OH_2)_5{}^{2+}$ using TD-DFT/B3LYP without spin−orbit coupling (see Computational Details). The resulting spectrum is shown in Figure 1. It should be noted that the spectrum refers to the pure electronic transitions, thus ignoring vibrational progressions that are prominent in the visible range of the absorption spectrum.[19] In view of the previous remarks concerning the accuracy of TD-DFT methods, the emphasis should be on the qualitative features of the spectrum.

The symmetry of the linear uranyl ion in the gas phase is $D_{\infty h}$, which is reduced to D_5 in the pentaaqua ion, where, strictly speaking, there is no inversion symmetry. However, the perturbing field from the coordinated water molecules is weak, and we therefore keep the $D_{\infty h}$ nomenclature. In the following discussion of the mechanism of the yl-exchange reactions given

(16) Farkas, I.; Bányai, I.; Szabó, Z.; Wahlgren, U.; Grenthe, I. *Inorg. Chem.* **2000**, *39*, 799–805.
(17) Wåhlin, P.; Danilo, C.; Vallet, V.; Réal, F.; Flament, J.-P.; Wahlgren, U. *J. Chem. Theory Comput.* **2008**, *4*, 569–577.
(18) Cao, Z.; Balasubramanian, K. *J. Chem. Phys.* **2005**, *123*, 114309.
(19) Kenney-Wallace, G. A.; Wilson, J. P.; Farrell, J. F.; Gupta, B. K. *Talanta* **1981**, *28*, 107–113.

by eqs 3–5, we will focus on the singlet electronic ground state $^1\Sigma_g^+$ and two excited triplet states, the lowest (luminescent) $^3\Delta_g(\sigma_u f_\delta)$ state at ~20 500 cm^{-1} and the higher $^3\Gamma_g$ state at ~36 000 cm^{-1}. We found that at the spin−orbit level, the luminescent state was 1_g with $^3\Delta_g$ character at the spin−orbit configuration interaction (SO-CI) level, while for SO-CASPT2 and SO-LR-CCSD, this state was 2_g with $^3\Phi_g$ character. However, the energy difference between 1_g and 2_g is small and essentially determined by the interplay between electron correlation and spin−orbit coupling between the $^3\Delta_g$ and $^3\Phi_g$ states. The transition probabilities to these excited states should be small, since they are spin- and parity-forbidden in the free ion, unless spin−orbit mixing with singlet states is strong. The calculated vertical energy of the $^3\Delta_g(\sigma_u f_\delta)$ state is close to the emission from the luminescent state and also to the first observed weak absorption band in the spectrum reported in Figures 3 and 4 of ref 19. As discussed by van Besien et al.,[20] the mixing between triplet and singlet states in the lower part of the spectrum, where the $(\sigma_u f_\delta)$ and $(\sigma_u f_\phi)$ configurations are located, is small. In a previous gas-phase study,[12] we found that the geometries of the uranyl(VI) ion in all of the excited states from the manifold corresponding to $(\sigma_u f_\delta)$ and $(\sigma_u f_\phi)$ electronic configurations [among which lies the luminescent $^3\Delta_g(\sigma_u f_\delta)$ state] are similar to that of the ground state, except that the U−O_{yl} distance is somewhat longer (by ~0.05 Å; see Table VII of ref 12). The situation is very different in the states with $(\pi_u f_\phi)$ and $(\pi_u f_\delta)$ electron configurations, where the two U−O_{yl} distances (1.72 and 1.93 Å) differ by 0.21 Å at the TD-DFT/B3LYP level (see Table VII of ref 12), resulting in a radical character for one oxygen, which should result in favorable proton/hydrogen acceptor properties. The chemical properties of the $^3\Delta_g(\sigma_u f_\delta)$ and $^3\Gamma_g$ states are thus very different, and this is the rationale for the exploration of the proton/hydrogen-transfer/yl-exchange reactions in these excited states. The radical states lie in the range 36000−38000 cm^{-1}, a region where there are many absorbing singlet states with $(\pi_u f_\phi)$, $(\pi_u f_\delta)$ configurations and small contributions from excitation out of the water molecule p orbitals. As mentioned earlier, these triplet and singlet states can mix as a result of spin−orbit coupling, making it possible to populate them and form an asymmetric photoexcited uranyl unit. In our models, we have taken the $^3\Gamma_g(\pi_u f_\phi)$ state as a representative of this manifold of "radical" states. When optimizing its equilibrium geometry, we did not encounter crossings with lower-lying electronic states (see below), suggesting that this state has a sufficiently long lifetime to undergo photochemical reactions. However, crossings appear in the proton/hydrogen transfer reaction, as will be discussed below.

Computational Details

Basis Sets and Relativistic Effective Core Potential. The uranium ion was described by a small-core relativistic effective core potential,[21] which includes 60 electrons in the core, and by the (12s11p10d8f)/[8s7p6d4f] contracted basis set.[21] No g polarization functions were included; Wåhlin et al.[17] and Vallet et al.[22] have shown that they have a small effect on the spectroscopy and energy barriers in reactions involving the uranyl aqua ion. All of the oxygen and hydrogen atoms were described at the all-electron level with valence triple-ζ plus polarization basis sets with

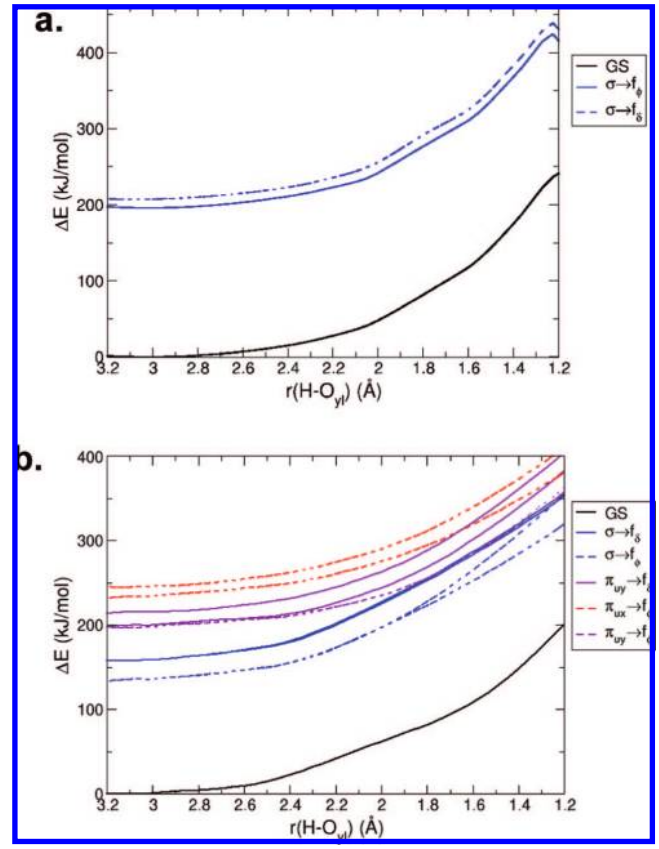

Figure 2. Energy profiles for $[UO_2(OH_2)]^{2+}$ computed at the TD-DFT/B3LYP level of theory along (a) the "σ" state reaction path, using geometries optimized for the "σ" state (TS obtained following the blue curve) and (b) the "π" state reaction path, using geometries optimized for the "π" state (TS obtained following the purple curve until the crossing with the blue manifold). Profiles of the ground state (GS) (black lines) and states of the "σ" manifold (blue lines) and "π" manifold (purple and red lines) are shown.

(11s6p1d)/[5s3p1d] and (5s1p)/[3s1p] contractions for oxygen[23] and hydrogen,[24] respectively.

Spin−Orbit-Free Calculations. The geometries at critical points along the reaction path were optimized using DFT for the electronic ground state and TD-DFT for the different excited states. The reaction path was followed using constrained optimizations, taking the distance between one of the yl-oxygens and the hydrogen of one coordinated water molecule as the reaction coordinate and relaxing all of the other degrees of freedom. The structure optimization of the different transition states (TSs) was possible for the ground state and the luminescent "σ" state configurations (using the automatic saddle-point optimization procedure) but not for the "π" state, for which the gradient optimization became difficult for H−O_{yl} distances shorter than 1.6 Å. The difficulties are illustrated by Figures 2b and 3b, which display the energy profiles for several states along the reaction path for the "π" state, using the optimized geometries. The potential energy surfaces corresponding to the same electronic configuration are parallel, generating multiple state crossings. Furthermore, at H−O_{yl} distances shorter than 1.6 Å, the manifold of "π" states is close to that of the "σ" states, resulting in failures of the optimization procedure. We thus estimated the structure of the transition state from geometries that could be optimized with constraints, assuming that the position of the transferred hydrogen could be extrapolated from the TS

(20) van Besien, E.; Pierloot, K.; Görller-Walrand, C. *Phys. Chem. Chem. Phys.* **2006**, *8*, 4311–4319.
(21) Küchle, W.; Dolg, M.; Stoll, H.; Preuss, H. *J. Chem. Phys.* **1994**, *100*, 7535–7542.
(22) Vallet, V.; Macak, P.; Wahlgren, U.; Grenthe, I. *Theor. Chem. Acc.* **2006**, *115*, 145–160.
(23) Schäfer, A.; Huber, C.; Ahlrichs, R. *J. Chem. Phys.* **1994**, *100*, 5829–5835.
(24) Schäfer, A.; Horn, H.; Ahlrichs, R. *J. Chem. Phys.* **1992**, *97*, 2571–2577.

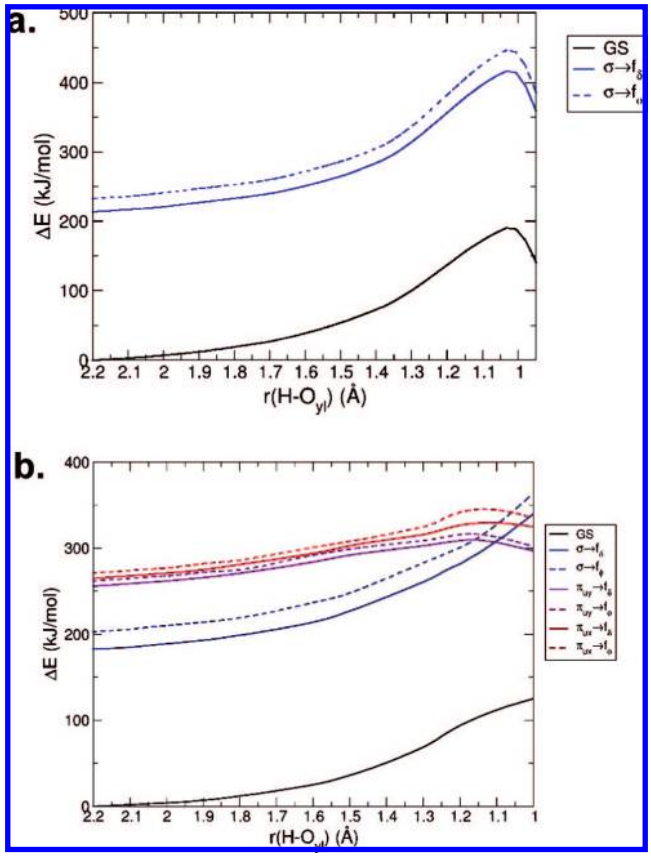

Figure 3. Energy profiles for $[UO_2(OH_2)_5]^{2+}$,(H_2O) computed at the TD-DFT/B3LYP level of theory along (a) the "σ" state reaction path, using geometries optimized for the "σ" state (TS obtained following the blue curve) and (b) the "π" state reaction path, using geometries optimized for the "π" state (TS obtained following the purple curve until the crossing with the blue manifold). Profiles of the ground state (black lines) and states of the "σ" manifold (blue lines) and "π" manifold (purple and red lines) are shown.

structure obtained for the "σ" state. A normal-mode analysis was carried out for all TS structures and showed the presence of a single imaginary mode with a frequency of ~500i cm^{-1} corresponding to the motion of the proton/hydrogen toward the yl-oxygen. The gradient-corrected B3LYP hybrid functional[25,26] was used, and the calculations were carried out using the Turbomole[27–30] and Gaussian packages.[31]

Solvent effects were estimated by single-point calculations using the conductor-like polarization model (CPCM)[32] with united force field (UFF) atomic radii[33] and the Gaussian package.[31] The perspective views of the molecular structures were made with CrystalMaker.[34]

Spin−Orbit Calculations. The influence of spin−orbit coupling on the energies of the reactant and the transition states for the reaction path involving $[UO_2(OH_2)]^{2+}$ was investigated in an SO-CI calculation using a configuration space that included the electronic configurations of all of the states of interest plus all singly excited (CIS) configurations that couple strongly to the reference configurations. This space allowed a good description of both spin−orbit-free orbital relaxation and spin−orbit polarization effects, but it did not describe electron correlation properly.

Table 1. Structures of the Reactants, Transition States, and Intermediates in the Proton/Hydrogen Transfer Reaction in the $^1\Sigma_g^+$ Ground State and the Two Excited States $^3\Delta_g(\sigma)$ and $^3\Gamma_g(\pi)$ of $[U^{VI}O_2(OH_2)]^{2+}$; The Structure of $[U^{V}O_2(OH_2)]^{+}$ Is Also Given[a]

	$[U^{VI}O_2(OH_2)]^{2+}$			$[U^{V}O_2(OH_2)]^{+}$
	GS	"σ" state	"π" state	GS
	Reactant			
r[U−O_{yl}(1)]	1.71	1.76	1.71	1.76
r[U−O_{yl}(2)]	1.71	1.76	1.94	1.76
r(U−O_{eq})	2.33	2.36	2.36	2.44
θ[O_{yl}(2)−U−O_{eq}]	90	90	89	89
	Transition State			
r[U−O_{yl}(1)]	1.70	1.76	1.72	
r[U−O_{yl}(2)]	1.78	1.81	1.95	
r(U−O_{eq})	2.17	2.20	2.34	
r[H−O_{yl}(2)]	1.20	1.25	"1.25"	
θ[O_{yl}(2)−U−O_{eq}]	65	64	58	
	Intermediate[b]			
r[U−O_{yl}(1)]	1.72	1.73	−	
r[U−O_{yl}(2)]	1.90	1.91	−	
r(U−O_{eq})	1.95	2.35	−	
r[H−O_{yl}(2)]	0.99	0.99	−	
θ[O_{yl}(2)−U−O_{eq}]	92	91	−	

[a] The structures of the ground and excited states were optimized at the DFT/B3LYP and TD-DFT/B3LYP levels of theory, respectively. Distances are in Å and angles in deg. [b] Because of electronic state crossing close to the TS, no optimization was performed for the "π" state intermediate (see the text for more details).

Correlation effects were included through an effective Hamiltonian approach (dressing) defined by the projection of the correlated spin−orbit-free TD-DFT energies onto the SO-CI space, as explained in refs 35 and 36. All of the SO-CI calculations were performed with the EPCISO code[36] interfaced to the MOLCAS quantum-chemistry package.[37]

Results

Proton/Hydrogen Transfer in the Pathway $[UO_2(OH_2)]^{2+}$ → $[UO_{yl}(OH)_{yl}(OH)_{eq}]^{2+}$. Structures and Energies of the Reactants, Transition States, and Intermediates. As a result of the state crossings shown in Figure 2b, the electronic state changes along the photochemical reaction path as follows: $[UO_2(OH_2)]^{2+}$ (π ground state) → $[UO_{yl}(OH)_{yl}(OH)_{eq}]^{2+}$ (π transition state) → $[UO_{yl}(OH)_{yl}(OH)_{eq}]^{2+}$ (σ intermediate).

The structures of the reactants for the proton/hydrogen transfer reactions in the $^1\Sigma_g^+$, $^3\Delta_g(\sigma_u f_\delta)$, and $^3\Gamma_g(\pi_u f_\phi)$ states were optimized without constraints; the results are given in Table 1. The bond distances in the ground state of $UO_2(OH_2)^{2+}$ are shorter than the experimental value[38] for the uranyl(VI) aqua

(25) Becke, A. D. *Phys. Rev. A* **1988**, *38*, 3098–3100.
(26) Lee, C.; Yang, W.; Parr, R. G. *Phys. Rev. B* **1988**, *37*, 785–789.
(27) Furche, F.; Ahlrichs, R. *J. Chem. Phys.* **2002**, *117*, 7433–7447.
(28) Furche, F.; Ahlrichs, R. *J. Chem. Phys.* **2004**, *121*, 12772–12773.
(29) Furche, F.; Rappoport, D. In *Computational and Theoretical Chemistry*; Elsevier: Amsterdam, 2005; Vol. 16, Chapter III.
(30) Rappoport, D.; Furche, F. *J. Chem. Phys.* **2005**, *122*, 064105.
(31) Frisch, M. J.; et al. Gaussian 03, revision D. 02; Gaussian, Inc.: Wallingford, CT, 2003.
(32) Barone, V.; Cossi, M. *J. Phys. Chem. A* **1998**, *102*, 1995–2001.
(33) Rappé, A. K.; Casewit, C. J.; Colwell, K. S.; Goddard, W. A., III; Skiff, W. M. *J. Am. Chem. Soc.* **1992**, *114*, 10024–10035.
(34) CrystalMaker, version 8.1; CrystalMaker Software Ltd.: Yarnton, U.K., 2008; http://www.crystalmaker.com.
(35) Llusar, R.; Casarrubios, M.; Barandiarán, Z.; Seijo, L. *J. Chem. Phys.* **1996**, *105*, 5321–5330.
(36) Vallet, V.; Maron, L.; Teichteil, C.; Flament, J.-P. *J. Chem. Phys.* **2000**, *113*, 1391–1402.
(37) Karlström, G.; Lindh, R.; Malmqvist, P.-Å; Roos, B. O.; Ryde, U.; Veryazov, V.; Widmark, P.-O.; Cossi, M.; Schimmelpfennig, B.; Neograd, P.; Seijo, L. *Comput. Mater. Sci.* **2003**, *28*, 222–239.
(38) Wahlgren, U.; Moll, H.; Grenthe, I.; Schimmelpfennig, B.; Maron, L.; Vallet, V.; Gropen, O. *J. Phys. Chem. A* **1999**, *103*, 8257–8264.
(39) Vallet, V.; Privalov, T.; Wahlgren, U.; Grenthe, I. *J. Am. Chem. Soc.* **2004**, *126*, 7766–7767.
(40) Brackett, F. P., Jr.; Forbes, G. S. *J. Am. Chem. Soc.* **1933**, *55*, 4459–4466.

Table 2. Activation Energies (ΔE_{TS}), Relaxation Energies (ΔE_{relax}), and Total Reaction Barriers to the Transition State ($\Delta E_{barrier}$) for the Proton/Hydrogen Transfer Reaction in the Ground, Luminescent, and Radical States of $UO_2(OH_2)^{2+}$ [a]

	ΔE_{TS}	ΔE_{relax}	$\Delta E_{barrier}$
GS	244	0	244
"σ" state	230	−20	210
"π" state	80	−95	−15

[a] Values are in kJ/mol and were computed at the DFT/B3YLP and TD-DFT/B3LYP levels of theory.

ion, but this is mainly a result of using a model with only one coordinated water; when the model with five coordinated water ligands was used, the agreement with experiment was much better (see Table 3). Geometry optimizations of the $^3\Delta_g$ state yielded a similar symmetric structure, although with U−O_{yl} distances longer than those in the ground state by 0.05 Å. The optimized structure of the $^3\Gamma_g$ state is distorted along the uranyl axis, with one of the U−O_{yl} bonds 0.23 Å longer than the other.

During the proton/hydrogen transfer reaction, the molecular orbitals of the system are mixed, and it is no longer meaningful to use labels from the linear triatomic molecule. To facilitate our discussion, we will use the following nomenclature: GS for the ground state, "σ" for the luminescent state, and "π" for the state corresponding to $^3\Gamma_g$ in the bare ion. The TS energies relative to the energies of the relaxed ground states (ΔE_{TS}) in the GS, "σ", and "π" reaction pathways are reported in Table 2, and the TS for the GS pathway is depicted in Figure S1 in the Supporting Information. The activation energies ΔE_{TS} for the GS and the fluorescent "σ" state are significantly larger than that for the "π" state, indicating that the latter provides a more favorable reaction pathway. It should be noted that the energy decreases for the "π" state when the H−O_{yl}(2) bond is stretched (see Figure 3b), and the estimated H−O_{yl} distance (see Computational Details) thus cannot be too short. This argument leads to the conclusion that the barrier for the "π" complex is probably slightly overestimated, but it is unlikely that this error will be important when discussing the relative magnitudes of the barriers along the three different pathways. The bond distances and angles at the TS are shown in Table 1, and the main difference between them is a longer r(U−O_{eq}) distance and a smaller O_{yl}(2)−U−O_{eq} angle for the "π" state. The presence of state crossings close to the TS structure of the "π" state suggests that the molecular system may cross over to another potential energy surface after the TS to reach an intermediate structure.

For the "σ" and "π" states, we performed spin−orbit coupling calculations at the reactant and TS geometries (the ground state has a closed-shell configuration, and spin−orbit effects are therefore small). Our previous spin−orbit calculations on the bare uranyl-ion[12] indicated that spin−orbit coupling does not change the main character of the "σ" and "π" states and only results in a decrease in all of the energies by ∼60 kJ/mol (5000 cm^{-1}); the resulting effect on the barrier is thus negligible.

Energy Changes along the Reaction Paths in the Ground State and the "σ" and "π" States: Relaxation Energies after Absorption. In the previous section, we proposed that photocatalyzed yl-exchange between isotope-enriched $U^{17/18}O_2^{2+}$ and water takes place in the excited "π" state. In this section we will briefly discuss how this state can be reached. Preferred excitations from the ground state are spin- and parity-allowed, leading to very short-lived excited states that can transfer energy either back to the ground state as fluorescence or to other states via internal conversion and intersystem crossing. Details of these processes are beyond the scope of this study, and we will assume that the $^3\Delta_g$ and $^3\Gamma_g$ states can be populated either from higher excited levels or by direct vertical excitation from the ground-state geometry; we will also present experimental evidence that the $^3\Gamma_g$ state can be populated from the $^3\Delta_g$ state. After excitation, the molecule will relax from the Franck−Condon region toward the excited-state minimum. The relaxation energies (ΔE_{relax}) were computed with the TD-DFT/B3LYP method, and the results are given in Table 2. Given the large gradients along the internal degrees of freedom of the uranyl aqua ion, the dynamics on short time scales will be dominated by motions along them, leaving only a smaller part of the relaxation energy ΔE_{relax} depicted in Figure 4 to be transferred to other degrees of freedom of the molecule and to the bulk solvent. We therefore suggest that a significant part of that relaxation energy is available to the molecular system for use in passing the activation barrier. In the following, we will assume that the entire relaxation energy is transferred to the uranyl ion, where it is available for passing the energy barrier. For the GS and the "σ" state, the energy barriers obtained with the TD-DFT method are comparable and very high (>230 kJ/mol). The computed barrier in the "π" state (80 kJ/mol) is significantly lower, indicating that this reaction path is the more favorable one. The TD-DFT energy path pictured in Figure 2b shows a state crossing at an H−O_{yl} distance of 1.25 Å in the "π" pathway, and at that point, the reaction crosses over to the potential energy curve of the luminescent "σ" state, leading to the same intermediate as that of the "σ" pathway.

The relaxation energy from the geometry at the vertical transition to that of the vibration-relaxed excited state provides the "π" state with a maximum energy of 95 kJ/mol, while the corresponding energy for the "σ" is 20 kJ/mol (Table 2). Part of this energy is accessible for passing the activation barrier, and the minimum additional energies needed to pass the barriers ($\Delta E_{barrier}$) are then 244, 210, and −15 kJ/mol for the ground, "σ", and "π" states, respectively (Table 2). The first two values are high, indicating that these pathways are less favored than the "π" pathway.

Proton/Hydrogen Transfer in the $[UO_2(OH_2)_5]^{2+}$,(H_2O) → $[UO_{yl}(OH)_{yl}(OH_2)_4]^{2+}$,(OH) Model. In this model, we have assumed that the proton/hydrogen transfer reactions involve water in the second coordination sphere. The favored location of the second-sphere water molecule is as a bridge between two first-shell molecules.[17] We have used the same scheme as detailed in the previous section to study the proton/hydrogen abstraction reaction in the $[UO_2(OH_2)_5]^{2+}$,(H_2O) model, noting that in this case we also have a state crossing along the "π" pathway, as shown in Figure 3b. Structures and some important bond distances for the "π" pathway are shown in Figure 5. At the TS, hydrogen acts as a bridge between the outer-sphere water molecule and one yl-oxygen, and the bridge is supported by several strong hydrogen bonds (Figure 5b). Subsequent fast proton/hydrogen transfer reactions result in the formation of the σ intermediate $[UO_{yl}(OH)_{yl}(OH)_{eq}(OH_2)_4]^{2+}$,$(H_2O)$.

Structures of the Reactants and Transition States and Excited-State Relaxation Energies. The $[UO_2(OH_2)_5]^{2+}$,(H_2O) distances for the reactants and the transition states for the GS, "σ", and "π" states are reported in Table 3. As was found for the first model studied, the major differences between the structures of the reactants in the various electronic states were the U−O_{yl} distances. For the reactants in the GS and "σ" reactions, the two U−O_{yl} distances are equal, with respective

Table 3. Geometries for the Reactants and Transition States in the Proton/Hydrogen-Exchange Reactions in the Ground, "σ", and "π" States of $[UO_2(OH_2)_5]^{2+}$,(H_2O); The Geometry of the Ground State of $[UO_2(OH_2)_5]^{+}$,(H_2O) Is Also Given[a]

	$r(U-O_{yl})$	$r(U-O_w)$	$r(H-O_{yl})$	$r(H-O_{eq})$	$\theta(O_{yl}-U-O_w)$
		Ground State			
reactant	1.751, 1.748	2.464, 2.481, 2.515, 2.503, 2.492, **4.055**	3.420	–	60
TS	1.825, 1.742	2.286, 2.413, 2.492, 2.491, 2.495, **3.217**	1.050	1.303	41
intermediate	1.877, 1.758	2.507, 2.058, 2.508, 2.560, 2.551, **4.158**	1.220	–	15
		"σ" State			
reactant	1.795, 1.795	2.467, 2.466, 2.521, 2.495, 2.520, **4.372**	5.017	–	93
TS	1.857, 1.737	2.303, 2.442, 2.491, 2.501, 2.501, **3.242**	1.03	1.310	43
intermediate	1.891, 1.804	2.507, 2.067, 2.513, 2.576, 2.572, **4.135**	1.241	–	18
		"π" State			
reactant	1.982, 1.763	2.485, 2.493, 2.511, 2.512, 2.512, **4.336**	4.484	–	76
TS	1.924, 1.796	2.395, 2.357, 2.485, 2.493, 2.499, **3.259**	1.05	1.441	46
intermediate[b]	–	–	–	–	–
		$[UO_2(OH_2)_5]^{+}$,(H_2O)			
GS	1.804, 1.831	2.564, 2.569, 2.571, 2.572, 2.572, **3.670**	1.932	–	47

[a] Geometries were calculated at the DFT/BY3LP and TD-DFT/B3LYP levels of theory. The $U-O_w$ distance in bold for each state represents the distance between the uranium atom and the oxygen belonging to the second-sphere water molecule. Distances are in Å and angles in deg. [b] Because of electronic state crossing close to the TS, no optimization was performed (see the text for more details).

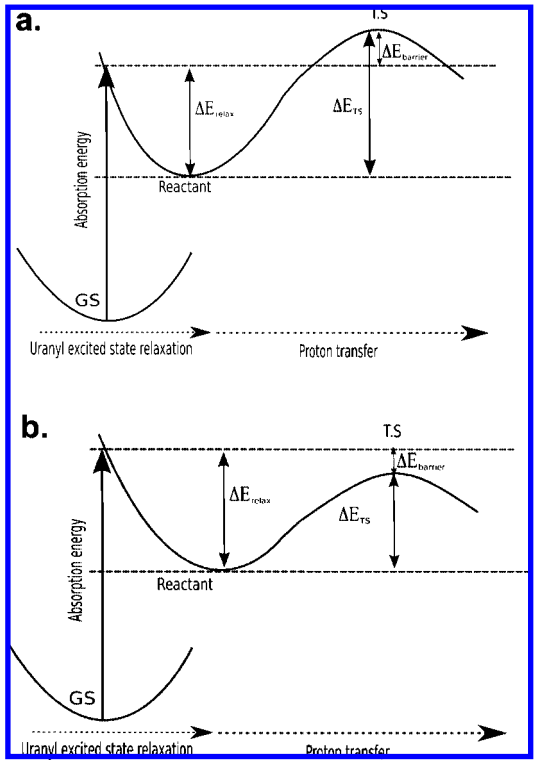

Figure 4. Schemes of the reaction path in the excited states: (a) the absorption energy is too low to overcome the barrier in the excited state; (b) the reaction can proceed.

values of 1.75 and 1.80 Å for these states; for the π state, the $U-O_{yl}$ distances are nonequivalent (1.98 and 1.76 Å). As all of the electronic states of interest involve electron-density changes localized on the uranyl unit, the equatorial water molecules have no large effect on the geometry; their role in the chemical reaction is in proton/hydrogen transfer.

The relaxation energies of the excited states computed with CPCM solvent effects (Table 4) were −12 and −86 kJ/mol for the "σ" and "π" states, respectively, almost identical to those obtained for both the bare uranyl ion (see Table VII of ref 12) and the simple chemical model (ΔE_{relax} in Table 2).

Reaction Profiles. The energy changes along the proton/transfer reaction path followed for the "σ" and "π" states at the TD-DFT/B3LYP level are shown in panels a and b, respectively, of Figure 3. The activation barriers are 210, 229, and 104 kJ/mol, respectively for the GS, "σ", and "π" states, respectively (Table 4). These calculated activation barriers in the gas phase are at most 30 kJ/mol lower than the corresponding values for the GS and "σ" states in the first model and 24 kJ/mol higher for the "π" state. In the CPCM model, the activation energies decreased by 24, 10, and 20 kJ/mol for the ground, "σ", and "π" states, respectively.

The activation barriers in the GS and "σ" states are high, even considering the contribution of −12 kJ/mol from energy relaxation in the "σ" state, making proton/hydrogen transfer less likely. The "π" reaction barrier (84 kJ/mol) is much lower. The maximum contribution from energy relaxation in the solvent is −86 kJ/mol, indicating that the energy barrier can easily be overcome; the "π" state is therefore the most probable route for protonation/hydrogenation, the formation of the intermediate $[UO_{yl}(OH)_{yl}(OH)_{eq}(OH_2)_4]^{2+}$, and finally yl-exchange with the solvent.

Hydroxide Interchange in the $[UO_{yl}(^{17/18}OH)_{yl}(OH)_{eq}(OH_2)_4]^{2+}$ Intermediate: The Second Step of the Exchange Reaction. In order to complete the yl-exchange reaction from the intermediate $[UO_{yl}(^{17/18}OH)_{yl}(OH)_{eq}(OH_2)_4]^{2+}$ (Figure 6a), the equatorial and axial hydroxide groups have to change places (Figure 6b); the equatorial OH group can then exchange with the solvent water. The reaction barrier for this step was computed at the DFT level in the ground state without any constraints and amounts to 20 kJ/mol in the gas phase and 22 kJ/mol in the CPCM solvent. This barrier is small, indicating a rapid site-exchange reaction.

Discussion

We will now discuss the details in the previous mechanistic model. We begin with the electronic state in which the photoinduced reaction might take place. In most of the experimental studies, the photoexcitation has been made in the UV region to higher spin-allowed singlet states, from which the energy may be dissipated back to the ground state as fluorescence or to higher triplet state(s) through internal conversion before the luminescent state is reached (see Scheme 1). It is not possible to elucidate the details of these processes or the relative contributions of radiation and radiationless processes. The quantum-chemical model that we have used allows us to

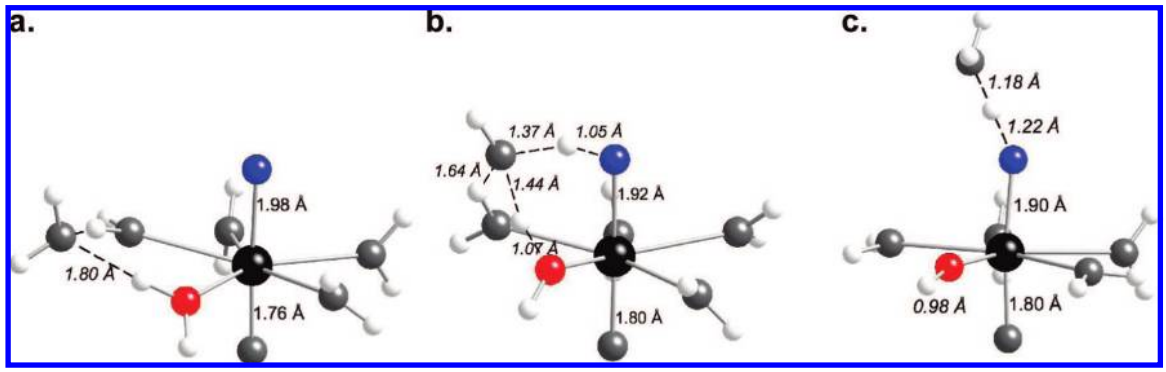

Figure 5. Perspective views of (a) the reactant, (b) the TS, and (c) the intermediate in the proton transfer mechanism in the "π" excited state of $[UO_2(OH_2)_5]^{2+}$,(H_2O). The intermediate (c) along this pathway is in the "σ" state as a result of state crossing. Panel (b) demonstrates the importance of hydrogen bonding in the TS and the "shuttle" function of the second-sphere water molecule in the hydrogen transfer.

Table 4. Activation Energies (ΔE_{TS}), Relaxation Energies (ΔE_{relax}), and Total Reaction Barriers to the Transition State ($\Delta E_{barrier}$) Computed in the Gas Phase and in the CPCM Solvent for the Proton/Hydrogen Transfer Reaction in the Ground, Luminescent "σ", and Radical "π" States of $[UO_2(OH_2)_5]^{2+}$,(H_2O)[a]

	gas phase			CPCM		
	ΔE_{TS}	ΔE_{relax}	$\Delta E_{barrier}$	ΔE_{TS}	ΔE_{relax}	$\Delta E_{barrier}$
GS	210	0	210	186	0	186
"σ" state	229	−10	219	219	−12	207
"π" state	104	−92	12	84	−86	−2

[a] Values are in kJ/mol and were computed at the DFT/B3YLP and TD-DFT/B3LYP levels of theory.

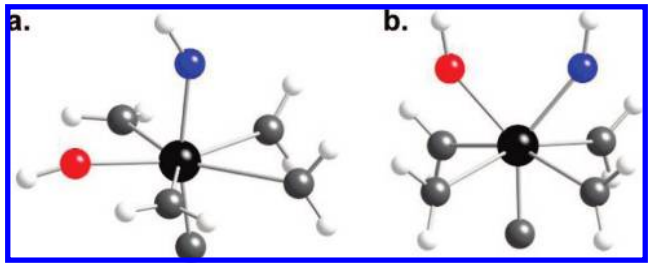

Figure 6. Perspective views of (a) the "σ" intermediate and (b) the TS for the exchange between axial and equatorial hydroxide groups in the ground state of $[UO_{yl}(OH)_2(OH_2)_4]^{2+}$.

Scheme 1

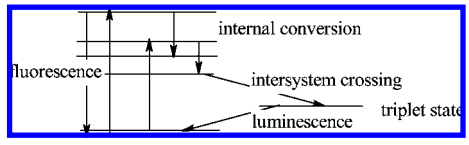

gain some insight into the electronic and chemical nature of the ground, luminescent "σ", and "π" states.

Chemical Character of the Various Electronic States. Excitations from the bonding orbitals to the f_δ and f_ϕ orbitals result by definition in electron transfer to the 5f nonbonding orbital centered on uranium, making this somewhat similar to UO_2^{+}. To illustrate this and to obtain a qualitative picture of the electron distribution, we have reported in Table S2 in the Supporting Information the Mulliken population analyses for both $[UO_2(OH_2)^{2+}]$* and $[UO_2(OH_2)]^{+}$. The uranium effective charge in the "σ" state of $[UO_2(OH_2)^{2+}]$* is identical to that of $[UO_2(OH_2)]^{+}$. This is due to transfer of ~0.48 electrons from the two yl-oxygens to the uranium center. In the "π" state, the charge transfer is even more pronounced (0.79 electrons) but now originates from the more distant yl-oxygen, $O_{yl}(2)$. The latter becomes positively charged, indicating that it acquires a radical character. This is also illustrated by the spin densities (see Figure 1 of ref 12), which show the localization of one of the electrons on the uranium and the other one on the more distant yl-oxygen. The other yl-oxygen, $O_{yl}(1)$, has the same charge as in the electronic ground state. At the TS, the H-accepting $O_{yl}(2)$ gains ~0.35 electrons from the equatorial oxygen. This indicates that the reaction in the "π" state may be seen as a hydrogen transfer rather than a proton transfer.

In the uranyl pentaaqua ion model, the Mulliken populations (Table S3 in the Supporting Information) in the reactant structures of the GS, "σ", and "π" states are also similar to those obtained for the simple chemical model (Table S2 in the Supporting Information), confirming that photoexcited uranyl can indeed be seen as a uranyl cation radical. Except for the U−O_{yl} distances, the bond distances in the "σ" and "π" states (Table 3) are shorter than those in $UO_2(OH_2)_5^{+}$ by 0.07 Å (see Table 3 and ref 39), indicating a geometry significantly different from that in UO_2^{+}. The more distant yl-oxygen in the "π" state has a positive charge in the relaxed structure in both models, indicating that it might be more prone to bind hydrogen than a proton. In the TS, however, the electron redistribution results in a negative charge on the yl-oxygen. From the population analysis of the two models, it seems difficult to draw any definite conclusions as to whether the exchange reaction involves hydrogen abstraction or proton transfer, so we must leave this question open.

Chemical Reactivity of the Different States. The energy barrier for the proton/hydrogen transfer in the electronic ground state of the uranyl pentaaqua ion is estimated as 186 kJ/mol (Table 4), which is significantly higher than the experimental value of 80 ± 14 kJ/mol reported by Szabó and Grenthe[2] for yl-exchange in the binuclear complex $(UO_2)_2(OH)_2^{2+}$. They found no evidence for thermal yl-exchange in the pentaaqua ion $UO_2(OH_2)_5^{2+}$, and the very high value of the calculated activation energy in the ground-state electron configuration is consistent with this experimental observation. The high activation energy of 219 kJ/mol for the luminescent state "σ" state (Table 4) implies that proton/hydrogen transfer does not take place in this state. The relaxation energy is small (~12 kJ/mol), and it seems unlikely that proton/hydrogen transfer can take place in higher vibrational states, as this would require an additional 207 kJ/mol (~17 000 cm^{-1}), corresponding to an excitation of ~37 000 cm^{-1}. Excitation with an energy of 32 000 cm^{-1} (312 nm) brings the system to the "π" state. The relaxation

energy is 86 kJ/mol (Table 4), which is 2 kJ/mol more than the computed energy barrier for proton/hydrogen transfer. This makes the latter process energetically accessible and explains the observed rapid photoactivated yl-oxygen exchange.[6b,15] The yl-exchange model that we have discussed involves several consecutive reactions, the important ones being proton transfer to form the corresponding intermediate and the subsequent exchange between equatorial and axial OH groups. As discussed previously, it is not possible to calculate the contribution of the relaxation energy to the "effective" energy barrier, and accordingly, we cannot decide the magnitude of the energy barrier for the hydrogen back-reaction or the lifetime of the intermediate $[UO_{yl}(^{17/18}OH)_{yl}(OH)_{eq}(OH_2)_4{}^{2+}]^*$,$(H_2O)$. In view of the large stability of the σ intermediate ($\sim$100 kJ/mol), it seems likely that the energy barrier for the back-reaction is large, which implies that there will be no significant back-reaction, as also indicated by the experimental results. The large relaxation energy may also result in a "concerted" formation of the σ intermediate in a one-step reaction. We will now discuss some of the previous mechanistic suggestions in the light of the conclusions from the present theoretical study. Scheme 1 outlines the possible events that can occur after photoexcitation of the uranyl(VI) ion.

Most of the experimental photochemical studies in which mechanistic interpretations have been discussed have used excitation in the range 390−440 nm (22700−25600 cm^{-1}). A large number of studies have also been made using UV irradiation, such as photooxidation as in actinometers (e.g., refs 40 and 5b). In all of these studies, it has been assumed that the photochemical reaction takes place in the luminescent triplet state. However, it is quite clear that excitation in the 390−440 nm range is not sufficient to reach the $^3\Gamma_g(\pi_u f_\phi)$ state.

There are two suggestions in the literature for the primary photoassisted reaction in one of the long-lived excited states: either a photoredox reaction (eq 1)[6] or direct proton/hydrogen abstraction from water (eq 2).[5d,7] In both models, OH radicals ($OH^\bullet$) are formed, but there is no unequivocal evidence for their presence in acidic solutions of $UO_2{}^{2+}$. It is not possible to distinguish between the two models on the basis of the experimental data. The quantum-chemical results in our study indicate that the photoexcited uranyl ion in the "σ" and "π" states has some characteristics of the $UO_2(OH_2)_5{}^+$ ion, but not surprisingly, there are significant differences, such as two different $U-O_{yl}$ distances and slightly longer $U-OH_2$ distances (see Table 3 and ref 39).

Mechanisms for the Photoinduced Yl-Exchange Reaction. The most detailed quantitative analyses of the experimental data have been given by Okuyama et al.[15] and Gaziev et al.,[6b] but the stoichiometric reaction mechanisms and rate constants proposed in these studies differ significantly from each other. Their experimental method did not permit any conclusions to be drawn concerning the nature of the photoreactive state, and in both studies, the authors assumed that it is the luminescent state; in addition, Gaziev et al.[6b] assumed that the reaction results in the formation of $UO_2{}^+$, which is not consistent with other experimental observations (see pp 1929−1932 of ref 5d). It is not possible to make any quantitative comparison between the results of our calculations and the experimental rates of exchange, but the identification of the absorption spectrum for a reactive intermediate in the study of Okuyama et al.[15] is consistent with our finding that the photochemical exchange reaction takes place in a triplet state above the luminescent one. Okuyama et al.[15] concluded that the absorption spectrum of the intermediate is not consistent with that of $UO_2{}^+$ in an aqueous solution. We agree and suggest that the absorption maximum corresponds to a spin-allowed transition from the luminescent $^3\Delta_g(\sigma_u f_\delta)$ state to the $\pi_u f_{\delta\phi}$ manifold localized at $\sim$36000−40000 cm^{-1} ($\sim$15000−19000 cm^{-1}) above the luminescent state. The lifetime of the luminescent state is certainly long enough to allow such a transition (the excitation source at 436 nm corresponds to 22 900 cm^{-1}) to one of these higher states. As these states have a radical character, the yl-exchange reaction can take place as suggested in the quantum-chemical calculations. In these higher-energy states, it seems feasible to have energy transfer between $[^{16}OU^{16}O^{2+}]^*$ and $[^{16}OU^{18}O]^{2+}$, as suggested by Okuyama et al.;[15] the former species acts as "sensitizer" for the isotope exchange, which takes place only through $[^{16}OU^{18}O^{2+}]^*$.

Conclusions

We have used quantum-chemical methods to investigate the yl-exchange reaction in both the ground and photoexcited uranyl(VI) ion. We have studied a chemical model in which the first step involves a proton/hydrogen transfer from an outer-sphere water molecule. The reaction was explored using the DFT and TD-DFT methods; even though these methods are less precise for calculation of reaction energies and spectra of actinide complexes, they are sufficiently good for predicting trends and differences in reactivity among various complexes or excited states, provided that these differences are large, as in the case discussed in the present report.

Our quantum-chemical results predict that the energy barrier for yl-exchange is very high in the ground state, in agreement with experimental data that show no isotope exchange between $UO_2{}^{2+}$(aq) and the water solvent in highly acidic aqueous solution.[2,6b] The quantum-chemical results show that the energy barrier is also very high in the long-lived luminescent state but much lower in the energetically accessible higher excited states located at $\sim$34000−40000 cm^{-1}, allowing the reaction to take place. This is at variance with many statements in the literature claiming that yl-exchange and other photochemically induced reactions take place in the luminescent state. On the basis of the experimental identification of a reaction intermediate by Okuyama et al.,[15] we suggest that the reactive excited states can be reached both by energy absorption from the luminescent state, which has a sufficiently long lifetime for such a process, and by direct excitation in the UV range. It seems experimentally feasible to check the proposal that the photochemical reaction takes place in a triplet state above the luminescent state through the use of a two-laser system in which one laser is used to populate the luminescent state and the second to study the energy absorption of this state. If the lifetime of the intermediate $[UO_{yl}(^{17/18}OH)_{yl}(OH)_{eq}(OH_2)_4]^{2+}$ is in the nanosecond range or longer, it also seems feasible to use the two-laser system to probe the vibrational spectrum of the photoexcited intermediate. The primary photochemical reaction in the "σ" and "π" states results in the formation of a cation radical that has some characteristics of $UO_2(OH_2)_5{}^+$ but is definitively a different species. On the basis of the population analysis, it seems difficult to decide if the reaction discussed involves hydrogen abstraction or proton transfer.

Acknowledgment. The authors thank Pernilla Wåhlin for very fruitful discussions. This study was made within two joint projects (JRP 01-12 and JRP 06-11) within the EC-supported ACTINET Network of Excellence. It was also supported by generous grants

from SKB, the Swedish Research Council, and the Carl Trygger Foundation. Laboratoire de Physique des Lasers, Atomes et Molécules is Unité Mixte de Recherche du CNRS. Computational resources were provided by the National Supercomputer Center in Linköping, Sweden (Project 007-05-36), the Centre de Ressources Informatiques (CRI), the Institut de Développement et de Ressources en Informatique Scientifique du Centre National de la Recherche Scientifique (IDRIS-CNRS) (Contract No. 71859), and the Centre Informatique National de l'Enseignement Supérieur (CINES) (Project phl2531).

Supporting Information Available: Structures of the reactant, transition state, and intermediate of the studied reaction for $[UO_2(OH_2)]^{2+}$ in the electronic ground state (Figure S1); structures of the reactant, transition state, and intermediate in the proton-transfer mechanism in the "σ" excited state of $[UO_2(OH_2)_5]^{2+}$,(H_2O) (Figure S2); vertical absorption energies and oscillator strengths for the uranyl pentaaqua ion (Table S1); Mulliken population analyses of the various species discussed for the simple chemical model and the uranyl pentaaqua ion model (Tables S2 and S3, respectively); Cartesian coordinates of the species discussed in the text; and complete ref 31. This material is available free of charge via the Internet at http://pubs.acs.org.

JA8026407